Design and Experiments of a High-Conversion-Efficiency 5.8-GHz Rectenna

James O. McSpadden, *Student Member, IEEE*, Lu Fan, *Member, IEEE*, and Kai Chang, *Fellow, IEEE*

***Abstract*—A high-efficiency rectenna element has been designed and tested at 5.8 GHz for applications involving microwave-power transmission. The dipole antenna and filtering circuitry are printed on a thin duroid substrate. A silicon Schottky-barrier mixer diode with a low breakdown voltage is used as the rectifying device. The rectenna element is tested inside a waveguide simulator and achieves an RF-to-dc conversion efficiency of 82% at an input power level of 50-mW and 327-Ω load. Closed-form equations are given for the diode efficiency and input impedance as a function of input RF power. Measured and calculated efficiency results are in good agreement. The antenna and circuit design are based on a full-wave electromagnetic simulator. Second harmonic power levels are 21 dB down from the fundamental input power.**

***Index Terms*—Detectors, nonlinear circuits, power conversion, rectennas, rectifying antennas.**

I. Introduction

OVER 100 years ago, the concept of wireless power transmission began with the ideas and demonstrations by Tesla [1]. Although Tesla was unsuccessful at implementing his wireless power transmission systems for commercial use, he did transmit power from his oscillators that operated up to 100 MV at 150 kHz. For demonstration purposes, Tesla would hold lighted light bulbs, which derived power from the uncollimated radiated energy. After Tesla's experiments, researchers in Japan [2] and the U.S. [3] continued efforts to promote wireless power transmission in the 1920's and 1930's.

The modern era of wireless power transmission began in the 1950's with the advancement of high-power microwave tubes by Raytheon Company, Waltham, MA [4]. By 1958, a 15-kW average power S-band cross-field amplifying tube was developed that had a measured overall dc-to-RF efficiency of 81% [5], [6]. The first receiving device for efficient reception and rectification of microwave power emerged in the early 1960's. Conceived at Raytheon, a rectifying antenna, or rectenna, was developed, consisting of a half-wave dipole antenna with a balanced bridge or single semiconductor diode placed above a reflecting plane. The output of the rectenna element is then connected to a resistive load. 2.45 GHz emerged as the transmitting frequency of choice due to its advanced and efficient technology base, location at the center of an industrial, scientific, and medical (ISM) band, and its minimal attenuation through the atmosphere even in heavy rainstorms.

The conversion efficiency of the rectenna continued to increase from the 1960's through the 1970's at 2.45 GHz. Conversion efficiency is determined by the amount of microwave power that is converted into dc power by a rectenna element. The greatest conversion efficiency ever recorded by a rectenna element occurred in 1977 by Brown, Raytheon Company [7]. Using a GaAs–Pt Schottky barrier diode, a 90.6% conversion efficiency was recorded with an input microwave-power level of 8 W. This rectenna element used aluminum bars to construct the dipole and transmission line. Later, a printed thin-film class of rectenna design was developed at 2.45 GHz where conversion efficiencies of 85% were achieved [8].

Components for microwave-power transmission have traditionally been focused at 2.45 GHz. To reduce the transmitting and rectenna aperture areas and increase the transmission range, researchers at ARCO Power Technologies, Inc., Washington, DC, developed a 72% efficient rectenna element at 35 GHz by 1991 [9]. 35 GHz was targeted due to a decrease in the atmospheric absorption around this frequency. However, components for generating high power at 35 GHz are expensive and inefficient.

To decrease the aperture sizes without sacrificing component efficiency, technology development at the next higher ISM band centered at 5.8 GHz has been investigated. This frequency is appealing for beamed power transmission due to smaller component sizes and a greater transmission range over 2.45 GHz.

In 1992, the first C-band rectenna achieved a 70% overall efficiency and a 80% conversion efficiency at 5.87 GHz [10]. These efficiencies were measured in a waveguide simulator with an input power level of approximately 700 mW per element. This C-band rectenna used a printed dipole, which fed a Si Schottky diode quad bridge. However, little information is provided on the design and testing of this rectenna.

In testing rectennas in a waveguide simulator, an overall efficiency (η_o) and conversion efficiency (η_c) are defined as

$$\eta_o = \frac{\text{dc output power}}{\text{incident RF power}}$$

$$\eta_c = \frac{\text{dc output power}}{\text{incident RF power-reflected RF power}}.$$

Measurements performed in a waveguide simulator can accurately monitor reflected power.

Manuscript received November 23, 1997; revised March 11, 1998. This work was supported in part by the NASA Center for Space Power, by the Army Research Office, and by the Texas Higher Education Coordinating Board's Advanced Technology Program.

J. O. McSpadden and K. Chang are with the Department of Electrical Engineering, Texas A&M University, College Station, TX 77843-3128 USA (e-mail: chang@eesun1.tamu.edu).

L. Fan is with Texas Instruments Incorporated, Dallas, TX 75243-4136 USA.

Publisher Item Identifier S 0018-9480(98)09037-1.

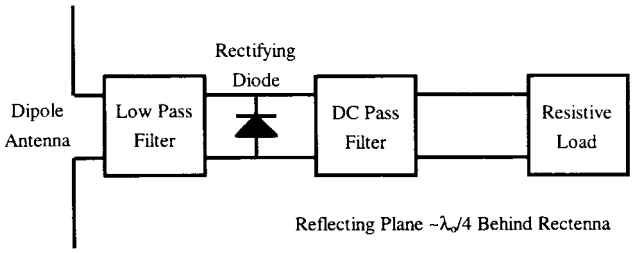

Fig. 1. The five main rectenna element components: antenna, input low-pass filter, rectifying diode, output filter, and resistive load.

The rectenna element in this paper operates efficiently (>80%) at much lower incident power levels of 20–65 mW with little reflected RF power (i.e., the overall efficiency is 1% lower than the conversion efficiency) [11]. This characteristic has two important applications in microwave-power beaming systems: 1) power can be converted efficiently at the edge of the rectenna where power densities are lower than the center elements and 2) power can be converted efficiently when the transmission distance is large and power density is low.

This rectenna is the first to be designed using a full-wave electromagnetic simulator. Previous rectennas have been designed using transmission-line models, Touchstone, and Libra [10], [12], [13]. A full-wave simulator allows the rectenna's antenna and passive circuit to be analyzed together. Also, closed-form equations for diode efficiency and input impedance agree well with the measured results.

II. Rectenna-Element Theory of Operation

Fig. 1 shows the main components of the rectenna element. A half-wave dipole attaches to a low-pass filter, which transforms the dipole impedance to the diode impedance and rejects higher order diode harmonics from radiating through the dipole. A diode placed in shunt across the transmission line is the rectifier. The output filter consisting of a large capacitor effectively shorts the RF energy and passes the dc power. The distance between the diode and output capacitor is used to resonate the capacitive reactance of the diode. Both input and output filters are used to store RF energy during the off period of the diode. A resistor is then placed across the output terminals to act as the load for measuring the output dc power. Finally, a reflecting metal plane is then placed behind the rectenna, typically 0.2–0.25 λ_o.

The typical operation of a rectenna element can be better understood by analyzing the diode's dc characteristics with an impressed RF signal. Fig. 2 shows an idealized RF voltage waveform V operating across the diode and the diode junction voltage [13], [14]. This simple model assumes that the harmonic impedances seen by the diode are either infinite or zero to avoid power loss by the harmonics. Thus, the fundamental voltage wave is not corrupted by higher order harmonic components. The rectenna conversion efficiency then depends only on the diode electrical parameters and the circuit losses at the fundamental frequency and dc. A mathematical model of the diode efficiency has been derived under this condition [13] and expanded to account for varying input power levels.

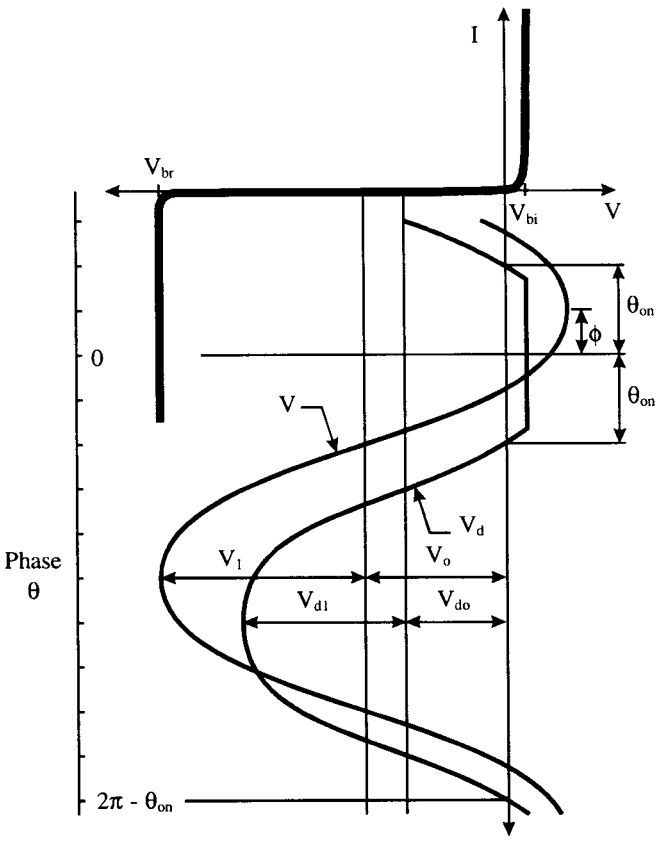

Fig. 2. Rectification cycle represented by the input fundamental and diode junction voltage waveforms impressed on the diode IV curve. This model assumes there are no losses in the harmonics and $\theta = \omega t - \phi$.

The diode junction waveform can be expressed as

$$V = -V_o + V_1 \cos(\omega t) \tag{1}$$

$$V_d = \begin{cases} -V_{do} + V_{d1} \cos(\omega t - \phi), & \text{if diode is off} \\ V_{\rm bi}, & \text{if diode is on} \end{cases} \tag{2}$$

where V_o is the output self-bias dc voltage across the resistive load and V_1 is the peak voltage amplitude of the incident microwave signal. Similar to mixers, the rectenna is a self-biasing circuit. As the incident power increases, the output dc voltage becomes more reversed biased. V_{do} and V_{d1} are the dc and fundamental frequency components of the diode junction voltage, and $V_{\rm bi}$ is the diode's built-in voltage in the forward bias region. Also shown in Fig. 2 are the forward-bias turn-on angles $\theta_{\rm on}$ of V_d and the phase difference ϕ between V and V_d. $\theta_{\rm on}$ is a dynamic variable dependent on the diode's input power and is determined by

$$\tan\theta_{\rm on} - \theta_{\rm on} = \frac{\pi R_s}{R_L\left(1 + \dfrac{V_{\rm bi}}{V_0}\right)} \tag{3}$$

where R_s is the diode's series resistance and R_L is the dc load resistance.

Fig. 3 shows the equivalent circuit of the diode used for the derivation of the mathematical model. The diode parasitic reactive elements are not included in the equivalent circuit. Instead, it is assumed they belong to the rectenna's environment circuit. The environment circuit is defined as the circuit

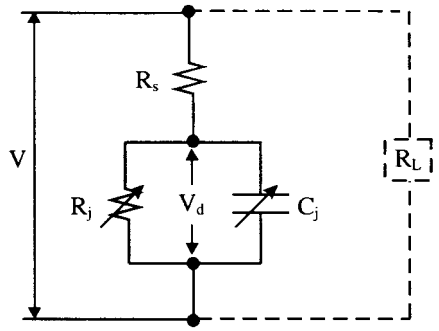

Fig. 3. Equivalent circuit model of the rectifying circuit consisting of the rectifying diode and dc load resistor.

around the diode that consists of linear-circuit elements. The diode model consists of a series resistance R_s, a nonlinear junction resistance R_j described by its dc IV characteristics, and a nonlinear junction capacitance C_j. A dc load resistor is connected in parallel to the diode along a dc path represented by a dotted line to complete the dc circuit. The junction resistance R_j is assumed to be zero for forward bias and infinite for reverse bias. By applying Kirchoff's voltage law, closed-form equations for the diode's efficiency and input impedance are determined.

The diode RF-to-dc efficiency is expressed as

$$\eta_d = \frac{1}{1+A+B+C} \tag{4}$$

where

$$A = \frac{R_L}{\pi R_s}\left(1+\frac{V_{\rm bi}}{V_o}\right)^2\left[\theta_{\rm on}\left(1+\frac{1}{2\cos^2\theta_{\rm on}}\right)-\frac{3}{2}\tan\theta_{\rm on}\right] \tag{5}$$

$$B = \frac{R_s R_L C_j^2 \omega^2}{2\pi}\left(1+\frac{V_{\rm bi}}{V_o}\right)\left(\frac{\pi-\theta_{\rm on}}{\cos^2\theta_{\rm on}}+\tan\theta_{\rm on}\right) \tag{6}$$

$$C = \frac{R_L}{\pi R_s}\left(1+\frac{V_{\rm bi}}{V_o}\right)\frac{V_{\rm bi}}{V_o}\left(\tan\theta_{\rm on}-\theta_{\rm on}\right) \tag{7}$$

and ω is the angular frequency $(=2\pi f)$. The junction capacitance used in (6) is defined as

$$C_j = C_{jo}\sqrt{\frac{V_{\rm bi}}{V_{\rm bi}+|V_o|}} \tag{8}$$

where C_{jo} is the diode's zero bias junction capacitance.

The diode input impedance is expressed in (9), shown at the bottom of this page. Assuming the reactance will be eliminated, the diode input resistance is

$$R_d = \frac{\pi R_s}{\cos\theta_{on}\left(\dfrac{\theta_{on}}{\cos\theta_{on}}-\sin\theta_{on}\right)}. \tag{10}$$

Similar to efficiency, the diode's input resistance is also a dynamic variable dependent on the input microwave power.

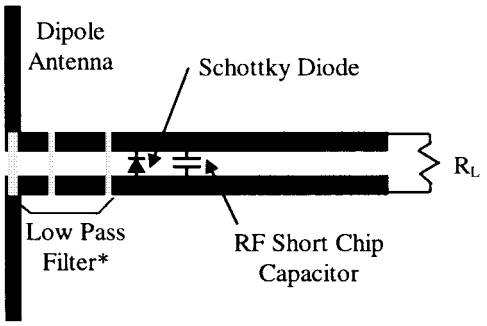

Fig. 4. 5.8-GHz rectenna element printed on an RT/Duroid 5880 substrate. The dipole antenna and CPS transmission line are printed on one side of the 10-mil (0.254 mm) substrate, and the low-pass filter is formed by strips printed on the opposite side. A reflecting plane is placed below the substrate approximately 0.21 λ_o.

III. Rectenna-Element Design

The 5.8-GHz printed rectenna element developed in this work is shown in Fig. 4. A two-plane structure is employed where the rectenna circuit is printed on a thin substrate and placed horizontally to a metal reflecting plane. Free space separates the substrate from the reflector. The sections that follow describe the steps taken to design the printed rectenna. The commercially available full-wave electromagnetic simulator IE3D is used to design the dipole antenna, coplanar stripline (CPS), and low-pass filter.[1]

A. CPS Characteristic Impedance

The horizontal dipole antenna and CPS transmission lines are printed on one side of 10-mil-thick (0.254 mm) Rogers 5880 duroid $(\varepsilon_r = 2.2)$ with 1-oz Cu (metal thickness = 0.035 56 mm). Based on the diode's package dimensions, the gap separation of the CPS is 2.1 mm and the printed lines are 1.6-mm wide.

Using IE3D, the simulated characteristic impedance at 5.8 GHz for a 2.1-mm gap (s) and 1.6-mm-wide strips (w) is approximately 236 Ω. The simulated effective dielectric constant $\varepsilon_{\rm eff}$ is 1.14 for the transmission-line structure composed of the duroid substrate separated by an 11-mm (0.21 λ_o) air gap above the reflector. Fig. 5 shows the simulated CPS characteristic impedance from 5–7 GHz. At 5.8 GHz, this simulated impedance is similar to the calculated impedance of 252 Ω using these parameters. The calculated impedance is given by [15]

$$Z_o = \frac{120\pi}{\sqrt{\dfrac{\varepsilon_{\rm eff}+1}{2}}}\,\frac{\pi}{\ln\left(2\dfrac{1+\sqrt{k'}}{1-\sqrt{k'}}\right)} \tag{11}$$

[1] IE3D, version 4.0, Zeland Software, Inc., Fremont, CA.

$$Z_d = \frac{\pi R_s}{\cos\theta_{\rm on}\left(\dfrac{\theta_{\rm on}}{\cos\theta_{\rm on}}-\sin\theta_{\rm on}\right)+j\omega R_s C_j\left(\dfrac{\pi-\theta_{\rm on}}{\cos\theta_{\rm on}}+\sin\theta_{\rm on}\right)} \tag{9}$$

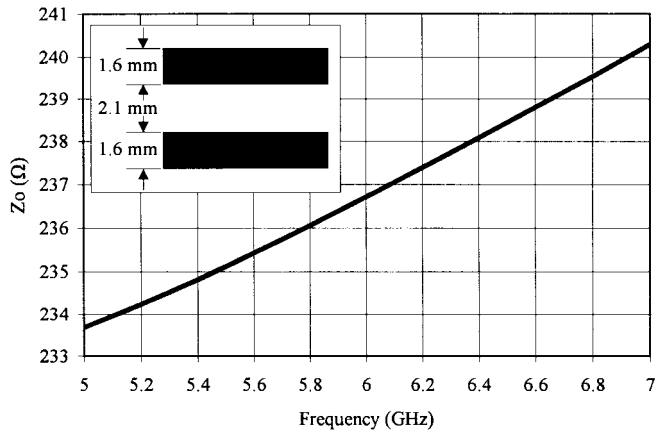

Fig. 5. Simulated CPS characteristic impedance determined by IE3D. The CPS is printed on a 10-mil-thick (0.254 mm) duroid substrate with a dielectric constant of 2.2 and a metal thickness of 1.4 mil (0.035 56 mm). The effective dielectric constant was simulated to be 1.14 by IE3D.

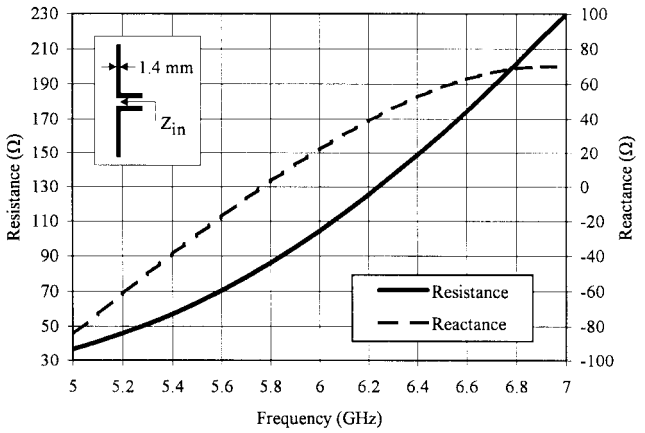

Fig. 6. Simulated input impedance of the 5.8-GHz dipole printed on a 10-mil-thick (0.254 mm) duroid substrate ($\varepsilon_r = 2.2$). The antenna is separated by 11 mm above a reflecting plane, and the dipole width and length are 1.4 mm and 25.75 mm, respectively. Resonance occurs at 5.8 GHz where the input resistance was determined to be 86 Ω.

where

$$k' = \sqrt{1 - \left(\frac{s}{s+2w}\right)^2} \tag{12}$$

$$s = 2.1 \text{ mm}$$

$$w = 1.6 \text{ mm}$$

$$\varepsilon_{\text{eff}} = 1.14 \text{ (from IE3D simulation)}.$$

The diode input impedance is taken to be 236 Ω to reduce the loss associated with the diode's built-in voltage. The efficiency loss caused by the forward V_{bi} drop across the Schottky barrier is approximately given by [7]

$$\text{Loss} = \frac{V_{\text{bi}}}{V_o + V_{\text{bi}}}. \tag{13}$$

Forcing the diode input impedance to be large will decrease the loss associated with V_{bi}.

B. Dipole Input Impedance

The simulated length and input resistance of the 5.8-GHz resonant dipole are approximately 25.75 mm and 86 Ω, respectively. Fig. 6 shows the simulated input impedance of the printed dipole by IE3D. Again, a 0.21-λ_o air gap separates between the horizontal dipole from the reflector. This simulated impedance is performed for the single element. In an actual rectenna array, mutual coupling effects would influence the impedance and would have to be considered.

C. Low-Pass Filter

The antenna terminals feed directly into a two-section low-pass filter. The low-pass filter performs the following two tasks: 1) match the input impedance of the dipole to the input impedance of the diode and 2) pass the 5.8-GHz operating frequency and reflect the higher order harmonics produced by the diode.

This filter design is based on the constant k class of low-pass filters [16]. Each of the two sections occupies a phase shift of 90° at 5.8 GHz. In this design, the second section performs the impedance transformation from the 86-Ω dipole impedance to the 236-Ω diode impedance. The equations used to design the low-pass filter result in capacitors that are physically large due to the thickness of the substrate. IE3D was used in an iterative process to reduce the capacitor areas while trying to achieve good low-pass filter characteristics. Fig. 7(a) shows the simulated results after reducing the capacitor values. At 5.8 GHz, the return loss on both dipole and diode ports is 16 dB. The simulated insertion loss is 0.2 dB at 5.8 GHz and 4 dB at the second harmonic frequency of 11.6 GHz. Fig. 7(b) shows the final lengths and capacitance values used in the design.

D. Rectifying Diode

An M/A-COM Si Schottky diode (MA40150-119) used for X-band mixer applications is the rectifying device. The measured built-in and breakdown voltages are approximately 0.4 and −8.8 V, respectively. As indicated earlier by the basic operation of the diode, this low breakdown voltage limits the diode's power handling capabilities. A maximum dc voltage of 4.4 is obtainable by this diode, but driving the diode at its extreme dc voltage limit could create an open circuit when the large reverse bias current flows through the diode. Typically, the breakdown voltage of a diode is divided by 2.2 to set the maximum output dc voltage. The zero-bias junction capacitance C_{jo} of this diode is 0.12 pF. An approximation of the diode series resistance is obtainable from the diode's *I–V* curve in the forward bias region. This resistance is estimated by the taking the inverse of the slope when the curve becomes mostly linear. Using this estimation, the MA40150-119 diode has a 8-Ω series resistance during the conducting portion of the cycle.

Fig. 8 provides an understanding of diode efficiency and diode input resistance as a function of dc load resistance. These curves are produced with $V_{\text{bi}} = 0$ and $C_j = C_{jo}$. Each dc load resistance represents a different θ_{on} as calculated from (3), and the varying θ_{on} is inserted into (4) and (10). The shaded region shows the range of dc loads where measured rectenna conversion efficiencies are greater than 80% at 5.8 GHz. Thus,

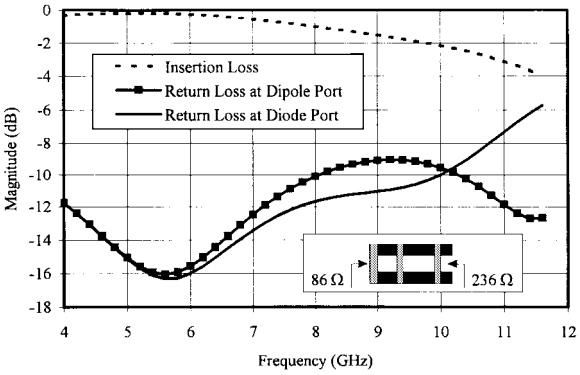

(a)

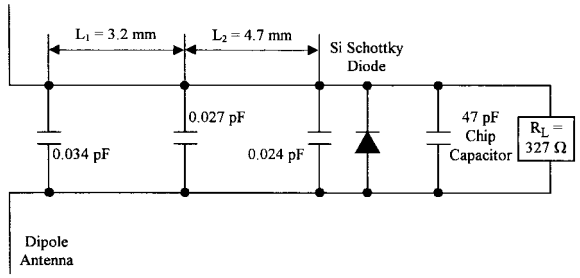

(b)

Fig. 7. (a) Simulated insertion and return losses of the optimized low-pass filter. A high frequency of 12 GHz and 40 cells per wavelength were used in the IE3D simulation. A good match to the 86-Ω dipole and 236-Ω CPS line is predicted at 5.8 GHz. (b) Final lengths and capacitance values used in the simulation.

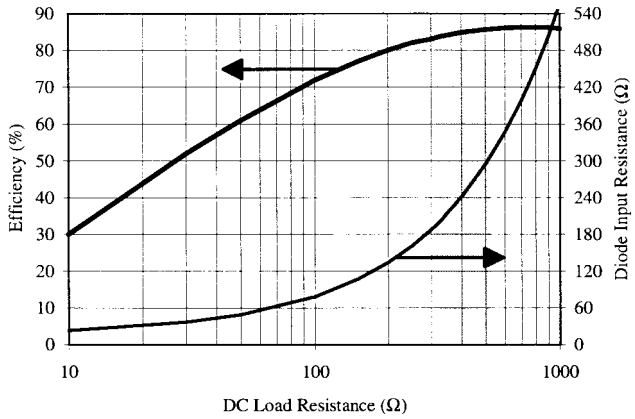

Fig. 8. Calculated diode efficiency and input resistance as a function of dc load resistance with $V_{\rm bi} = 0$ and $C_j = C_{jo}$. The shaded region shows the range of dc load resistances where the measured conversion efficiency is >80%.

it is possible to approximately determine the proper diode input resistance and load resistance to obtain a high efficiency based solely on the diode's C_{jo} and R_s.

E. Output RF Filter

A 47-pF chip capacitor is used to effectively short the RF energy and pass the dc power to a resistive load. The distance between the chip and diode is used to cancel the capacitive reactance of the diode. This resonance is needed to maximize the diode efficiency.

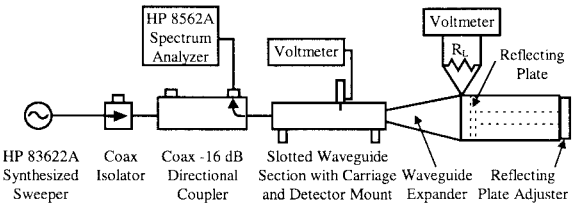

Fig. 9. Rectenna measurement setup. A coax cable connects the RF source to the coax isolator. The coax 16-dB directional coupler monitors the second-harmonic power level. A WR 137 slotted waveguide section on a carriage with a detector diode attached to a voltmeter is used to monitor standing waves in the system. A custom-made waveguide section expands the WR 137 to a square opening for the rectenna element to reside. A sliding short is placed in a square waveguide section behind the element to act as the reflecting plane. DC output power from the rectenna is monitored by a voltmeter connected across a resistor load.

F. Resistive Load

The resistive load at the output of the rectenna element is typically 1.3–1.4× the diode input resistance [16]. A load of 327 Ω resulted in the highest conversion efficiency at 1.39× the 236-Ω diode impedance. Output dc power is accurately measured by measuring the voltage across the resistor. This power level is limited by the diode's breakdown voltage as given by

$$P_{\rm dc} < \frac{V_{br}^2}{4R_L}. \tag{14}$$

IV. Rectenna-Element Measurements

A waveguide simulator was designed to test and evaluate the rectenna element. The short dimension of a standard WR 137 waveguide was expanded to equal the wide dimension. Thus, the rectenna is placed in a square opening (3.485 cm × 3.485 cm). Based on the cutoff frequency of the WR 137 waveguide and the operating frequency of 5.8 GHz, the angle of incidence is calculated to be 47.9° from boresight [17]. Thus, the rectenna efficiency proves to be very nondirectional. In applications where the rectenna is placed on a moving target, this aspect allows the rectenna to receive power efficiently at various angles of incidence.

Fig. 9 shows the measurement setup. The HP 83622A synthesized sweeper provides the RF input power and allows the power and frequency to be varied. In addition to built-in isolators of the sweeper, a coaxial isolator provides additional protection from the reflected energy. A coaxial directional coupler is inserted to measure the harmonic power generated by the rectenna element. The coupled port is connected to a spectrum analyzer to measure the harmonic power level. A coax-to-waveguide adapter is used to connect to a waveguide slotted line to monitor the reflected RF power. Voltage standing-wave ratio (VSWR) measurements by a voltmeter are taken using the mounted detector on the slotted-line carriage. The waveguide expander transitions from WR 137 waveguide to the square output of the waveguide simulator. The rectenna element is placed between the waveguide expander and a square waveguide section. This square waveguide houses an adjustable reflecting plane to tune the rectenna element.

Fig. 10 shows the measured overall and conversion efficiencies of the rectenna using a 327-Ω resistor load. The highest

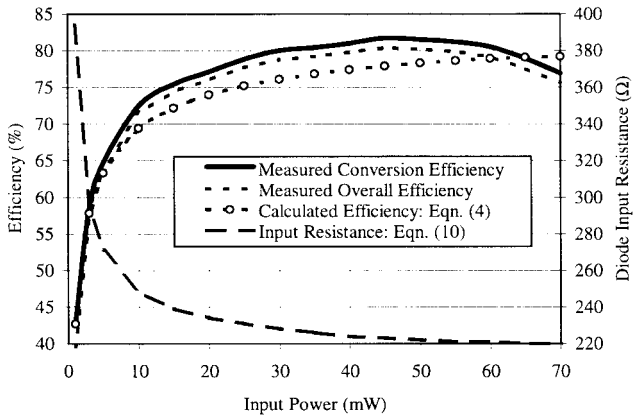

Fig. 10. Measured and calculated rectenna performance at 5.8 GHz with a 327-Ω load. A mismatch of the rectenna element with the system resulted in an efficiency decrease of 1% from the conversion to overall efficiency. A maximum conversion efficiency of 82% occurs at an input power of 50 mW. Also shown is the calculated diode input resistance as a function of input power.

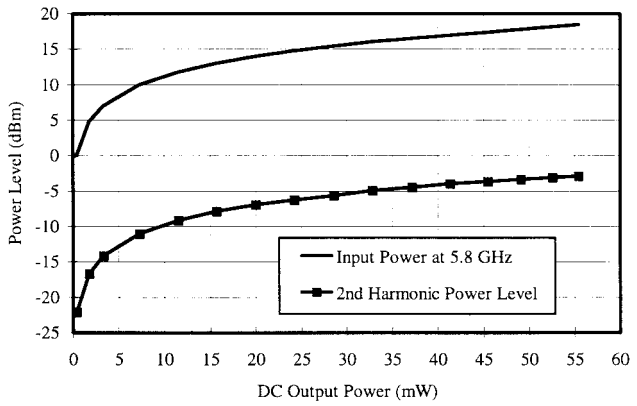

Fig. 11. Comparison of the measured second-harmonic radiation level relative to the fundamental input power. On average, the second harmonic is 21 dB down from the fundamental.

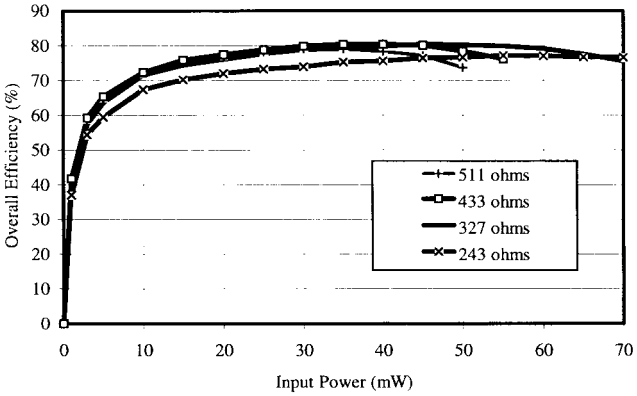

Fig. 12. Overall measured efficiency comparison of the 5.8-GHz rectenna with different resistive loads. The 327-Ω load gave the best match to the system with a VSWR of 1.29 at 50 mW of input RF power.

efficiency occurs when the rectenna substrate and reflecting plane are separated by 11.1 mm (0.21 λ_o). A maximum conversion efficiency of 82% is achieved at an input power of 50 mW. The differences between the overall efficiency and conversion efficiency indicate that little power (<1%) is reflected from the measurement system. Also shown is the calculated diode efficiency and input resistance. These calculated curves use the measured output dc voltage and the diode $V_{\rm bi}$ for calculating $\theta_{\rm on}$. The diode efficiency curve also relies on (8) to calculate C_j using the measured V_o. The maximum conversion efficiency of the rectenna element is measured to be 82% and the corresponding calculated diode efficiency is 78.3%. The mathematical model relies on a constant diode series resistance and a simple expression for junction capacitance. This 3.7% difference between measured and calculated efficiency is related to these factors. Also, the calculated diode input resistance varies from 220 to 228 Ω when the measured conversion efficiency is greater than 80%, which also will possess a certain degree of error. A more complex diode model could be developed to account for a varying series resistance, but this simple model agrees fairly well with the measured results.

Although filters are placed on the rectenna element to suppress the radiation of harmonics generated by the diode, this power will radiate into free space with this rectenna structure. Fig. 11 shows the measured second-harmonic power level created by the diode with respect to the fundamental input power. Similar to results of 2.45-GHz rectennas [7], the 11.6-GHz second-harmonic power level is on average 21 dB down from the 5.8-GHz input power. Fig. 9 shows the measurement system used to measure the second harmonic. The third harmonic was barely detectable with this system and was omitted. This measurement was performed by recording the power level of the second harmonic by a spectrum analyzer, while accounting for the system loss up to the input of the expanded waveguide section. The slotted waveguide section was removed for this measurement. Harmonic radiation can be further reduced by the addition of a frequency-selective surface (FSS) placed on top of the rectenna. An FSS has been previously developed for a 2.45-GHz rectenna that suppressed the second-harmonic radiation by 10 dB [18].

Fig. 12 shows the effects of varying the resistive load on the rectenna at 5.8 GHz. The range of loads used indicate very small changes in overall efficiency, as predicted by (4). Although the maximum conversion efficiencies associated with these overall efficiencies varies from 79% to 82%, they had a higher VSWR compared to the 327-Ω load. The 327-Ω load provided the best match to the system with a VSWR of 1.29 at an input power of 50 mW. The rectenna element converts power efficiently (>80%) even when the load varies from 300 to 500 Ω.

Fig. 13 shows the rectenna conversion efficiency when the frequency is varied at a constant input power of 50 mW and a resistive load of 327 Ω. Since the measurement system changes electrically with frequency, calibration took place by measuring the input power to the expanded waveguide section for each frequency. Changing the frequency influences the rectenna's performance by electrically changing the dipole impedance and reflecting plane spacing. These measurements were taken while changing the reflector plane spacing to achieve the highest conversion efficiency. As seen, a maximum

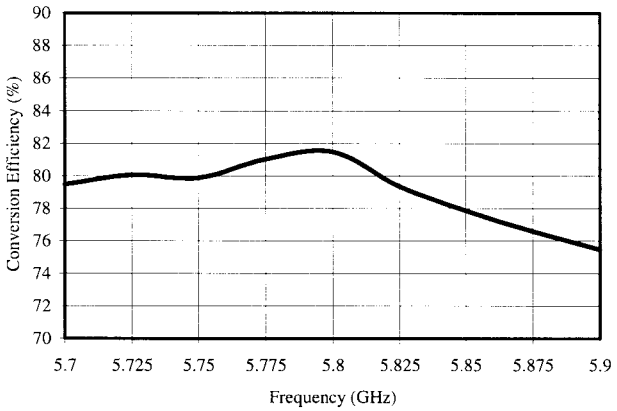

Fig. 13. Measured conversion efficiency of the rectenna at different frequencies. The spacing between the reflecting plane and rectenna is changed to maximize the output dc power at each frequency. The input power and resistive load at all frequencies are 50 mW and 327 Ω, respectively.

conversion efficiency of 82% occurs at 5.8 GHz. The efficiency remains above 77% over the entire ISM band located between 5.725–5.875 GHz.

V. Conclusions

A rectenna element has been developed which has the highest recorded conversion efficiency of 82% at 5.8 GHz with an input power of 50 mW. The rectenna has good impedance matching, and the reflected power is very small (VSWR <1.3). This results in an almost identical conversion efficiency and overall efficiency. Closed-form equations are given to approximate the diode efficiency and input impedance. The critical parameters of a highly efficient rectifying circuit include the diode R_s, C_{jo}, and V_{bi} and the dc load resistance R_L. The theory presented here shows the important relationships between these components to achieve a high conversion efficiency. The circuit design was based on electromagnetic and circuit analysis and accurately tested in a closed environment. This rectenna illustrates the importance of a full-wave simulator as a valuable asset in design.

Acknowledgment

The evaluation copy of IE3D by Zeland Software, Fremont, CA, is acknowledged by the authors.

References

[1] M. Cheney, *Tesla Man Out of Time.* Englewood Cliffs, NJ: Prentice-Hall, 1981.
[2] H. Yagi and S. Uda, "On the feasibility of power transmission by electric waves," in *Proc. 3rd Pan-Pacific Sci. Congr.*, vol. 2, Tokyo, Japan, 1926, pp. 1305–1313.
[3] "Electric light without current," *Literary Dig.*, vol. 112, no. 3, p. 30, Jan. 1932.
[4] W. C. Brown, "The history of power transmission by radio waves," *IEEE Trans. Microwave Theory Tech.*, vol. MTT-32, pp. 1230–1242, Sept. 1984.
[5] ——, "The amplitron: A super power microwave generator," *Electron. Progress*, vol. 5, no. 1, pp. 1–5, July/Aug. 1960.
[6] ——, "The history of the crossed-field amplifier," *IEEE MTT-S Newslett.*, no. 141, pp. 29–40, Fall 1995.
[7] ——, "Electronic and mechanical improvement of the receiving terminal of a free-space microwave power transmission system," Raytheon Company, Wayland, MA, Tech. Rep. PT-4964, NASA Rep. CR-135194, Aug. 1977.
[8] W. C. Brown and J. F. Triner, "Experimental thin-film, etched-circuit rectenna," in *IEEE MTT-S Int. Microwave Symp. Dig.*, Dallas, TX, June 1982, pp. 185–187.
[9] P. Koert, J. Cha, and M. Machina, "35 and 94 GHz rectifying antenna systems," in *SPS 91-Power from Space Dig.*, Paris, France, Aug. 1991, pp. 541–547.
[10] S. S. Bharj, R. Camisa, S. Grober, F. Wozniak, and E. Pendleton, "High efficiency C-band 1000 element rectenna array for microwave powered applications," in *IEEE MTT-S Int. Microwave Symp. Dig.*, Albuquerque, NM, June 1992, pp. 301–303.
[11] J. O. McSpadden, L. Fan, and K. Chang, "A high conversion efficiency 5.8 GHz rectenna," in *IEEE MTT-S Int. Microwave Symp. Dig.*, Denver, CO, June 1997, pp. 547–550.
[12] S. Adachi and Y. Sato, "Microwave-to-dc conversion loss of rectenna," *Space Solar Power Rev.*, vol. 5, no. 4, pp. 357–363, 1985.
[13] T. Yoo and K. Chang, "Theoretical and experimental development of 10 and 35 GHz rectennas," *IEEE Trans. Microwave Theory Tech.*, vol. 40, pp. 1259–1266, June 1992.
[14] W. C. Brown, "Free-space microwave power transmission study, combined phase III and final report," Raytheon Company, Waltham, MA, Tech. Rep. PT-4601, NASA Contract NAS-8-25374, Sept. 1975.
[15] K. C. Gupta, R. Garg, and I. J. Bahl, *Microstrip Lines and Slotlines.* Norwood, MA: Artech House, 1979, pp. 261–265.
[16] W. C. Brown, "Design definition of a microwave power reception and conversion system for use on a high altitude powered platform," Raytheon Company, Wallops Flight Facility, VA, NASA CR-156866, NASA Contract NAS 6-3006, July 1980, pp. 3-16–3-21.
[17] P. W. Hannan and M. A. Balfour, "Simulation of a phased-array antenna in waveguide," *IEEE Trans. Antennas Propagat.*, vol. AP-13, pp. 342–353, May 1965.
[18] J. O. McSpadden, T. Yoo, and K. Chang, "Theoretical and experimental investigation of a rectenna element for microwave power transmission," *IEEE Trans. Microwave Theory Tech.*, vol. 40, pp. 2359–2366, Dec. 1992.

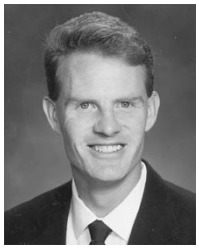

James O. McSpadden (S'88) was born in Denton, TX, on June 26, 1966. He received the B.S. and the M.S. degrees in electrical engineering and the Ph.D. degree from Texas A&M University, College Station, in 1989, 1993, and 1998, respectively.

From June 1989 to August 1990, he was with the Marathon Pipe Line Company, Houston, TX, as an Associate Engineer. While in graduate school, he was a Lecturer, Teaching Assistant, and Research Assistant. In 1993, he also attended the University of Alaska Fairbanks, as a Texas Space Grant Consortium Visiting Fellow. He is currently with Boeing Information, Space, and Defense Systems Group, Seattle, WA, where he is involved with phased-array antennas.

Dr. McSpadden is a member of Eta Kappa Nu and Tau Beta Pi.

Lu Fan (M'96) received the B.S. degree in electrical engineering from the Nanjing Institute of Technology (now Southeast University), Nanjing, China, in 1982.

From September 1982 to December 1990, he was with the Department of Radio Engineering, Nanjing Institute of Technology, as a Teaching Assistant and Lecturer. In January 1991, he became a Research Associate in the Department of Electrical Engineering, Texas A&M University, College Station. He is currently with Texas Instruments Incorporated, Dallas, TX. His interests include RF and microwave circuit design and testing.

Kai Chang (S'75–M'76–SM'85–F'91) received the B.S.E.E. degree from the National Taiwan University, Taipei, Taiwan, R.O.C., in 1970, the M.S. degree from the State University of New York at Stony Brook, in 1972, and the Ph.D. degree from the University of Michigan at Ann Arbor, in 1976.

From 1972 to 1976, he was with the Microwave Solid-State Circuits Group, Cooley Electronics Laboratory, University of Michigan at Ann Arbor, as a Research Assistant. From 1976 to 1978, he was with Shared Applications, Inc., Ann Arbor, MI, where he worked in computer simulation of microwave circuits and microwave tubes. From 1978 to 1981, he was with the Electron Dynamics Division, Hughes Aircraft Company, Torrance, CA, where he was involved in the research and development of millimeter-wave solid-state devices and circuits, power combiners, oscillators, and transmitters. From 1981 to 1985, he was with TRW Electronics and Defense, Redondo Beach, CA, as a Section Head, where he developed state-of-the-art millimeter-wave integrated circuits and subsystems, including mixers, voltage-controlled oscillators (VCO's), transmitters, amplifiers, modulators, upconverters, switches, multipliers, receivers, and transceivers. In August 1985, he joined the Electrical Engineering Department, Texas A&M University, College Station, as an Associate Professor, and was promoted to a Professor in 1988. In January 1990, he was appointed E-Systems Endowed Professor of Electrical Engineering. He has authored and co-authored *Microwave Solid-State Circuits and Applications* (New York: Wiley, 1994), *Microwave Ring Circuits and Antennas* (New York: Wiley, 1996), and *Integrated Active Antennas and Spatial Power Combining* (New York: Wiley, 1996). He served as the editor of the four-volume *Handbook of Microwave and Optical Components* (New York: Wiley, 1989, 1990). He is the Editor of the *Microwave and Optical Technology Letters* and the Wiley Book Series in Microwave and Optical Engineering. He has published over 300 technical papers and several book chapters in the area of microwave and millimeter-wave devices, circuits, and antennas. His current interests are in microwave and millimeter-wave devices and circuits, microwave integrated circuits, integrated antennas, wide-band and active antennas, phased arrays, microwave-power transmission, and microwave optical interactions.

Dr. Chang received the Special Achievement Award from TRW in 1984, the Halliburton Professor Award in 1988, the Distinguished Teaching Award in 1989, the Distinguished Research Award in 1992, and the TEES Fellow Award in 1996 from Texas A&M University.